# Experimental and Numerical Study on the Bead-Carry-Out in Two-Component Development Process in Electrophotography

*Nobuyuki Nakayama,* Yoichi Watanabe,* Yasuaki Watanabe,* and Hiroyuki Kawamoto***
**Research and Development Center, Fuji Xerox Co., Ltd., Kanagawa, Japan*
***Department of Mechanical Engineering, Waseda University Shinjuku, Tokyo, Japan*

## Abstract

Experimental and numerical investigations have been carried out on the bead-carry-out phenomenon of electromagnetic bead chains in two-component development process of electrophotography. Electrostatic pull-off characteristics were measured in a magnetic field and then it was clarified how the critical pull-off field intensity to break chains and the amount of pulled-off carriers depended on the bead diameter and the magnetic field. Magnetic bonding force and electrostatic pull-off force were estimated numerically to discuss these experimental results. It was clarified that the bead-carry-out phenomenon can be predicted qualitatively from the comparison of calculated magnetic force and electrostatic force.

## Introduction

A schematic drawing of a two-component development process[1] used for high-speed and/or color laser printers is shown in Fig. 1. Magnetized carrier beads in the magnetic field created by a stationary permanent magnet form chain clusters on the rotatory sleeve. Toner particles attached electrostatically to these magnetic bead chains are transported with rotation of the sleeve. In the development area, electrostatic force acts on toner particles and they move to photoreceptor surface to form real images.

It is well known as the bead-carry-out phenomenon (BCO) that the electrostatic force also acts on chains and bead(s) are separated from chains and moved to photoreceptor surface. The attached carrier bead(s) on the photoreceptor surface cause significant image degradations. To clarify the mechanism of BCO and to clarify requirements to prevent BCO are important, however very few studies had been reported.

In this study, experimental and numerical investigations have been carried out on the BCO phenomenon to clarify the mechanism and effects of parameters. In the experiment, a critical pull-off field intensity to separate bead(s) form chains formed on a solenoid coil were measured and effects of bead diameter and coil current were evaluated. Amount of pulled-off carriers was also measured in another experiment with a magnet roller. In addition, numerical simulation of chain formation was performed to estimate magnetic bonding force between the beads in the chain using Distinct Element Method (DEM). An electrostatic pull-off force was estimated by the electric field calculation of chains. These numerical results were compared to experimental results to discuss adequacy of the method and to study pull-off characteristics.

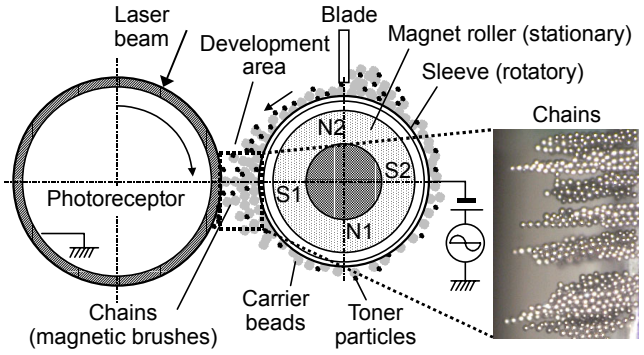


*Figure 1. Two-component development process for laser printers.*

## Experimental Method

**Solenoid Coil System**

Figure 2 shows an illustration and a photograph of the experimental setup with a solenoid coil[2,3] to simulate electrostatic pull-off phenomenon of chains. Spherical, soft magnetic, and conductive carriers were provided at the center of the end plate on the solenoid coil. These carriers are 35-107 μm in diameter, 3500-3620 kg/m$^3$ in volume density, 4.2-4.7 in relative magnetic permeability and the surface loading was 0.637 kg/m$^2$. Chains of carriers formed

in the magnetic field, as shown in Fig. 3, were observed by a digital microscope (Keyence Corp., VH-7000). Then the electric field was applied statically to the chains between a set of parallel electrodes with 6.0 mm in gap. If the sufficient electric field is applied, carrier beads at the top of chains were charged and pulled off by the electrostatic force. The critical voltage between electrodes to break chain was recorded.

Axial magnetic flux density $B'$ along the center axis of the coil was measured and approximated by $B'(z) = B_0(1-cz)$, where $B_0$ and $c$ (= 66.9 1/m) are constants and $z$ is the axial coordinate. ($z = 0$ at the surface of the end plate on which carrier beads were mounted.) $B_0$ is proportional to the coil current with a proportional constant 6.16 mT/A.

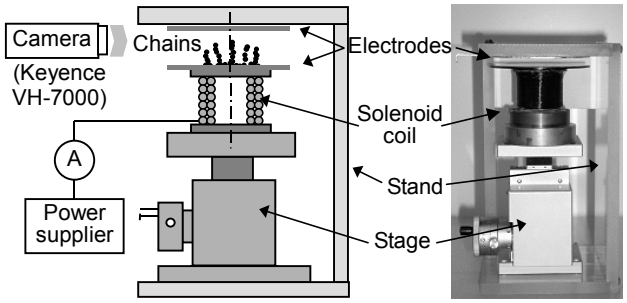


*Figure 2. Experimental setup with solenoid coil.*

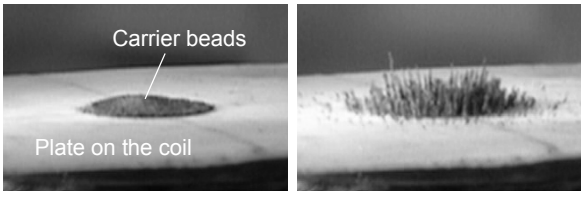


(a) Without magnetic field (b) With magnetic field

*Figure 3. Photographs of magnetic carrier beads with and without magnetic field created by a coil.*

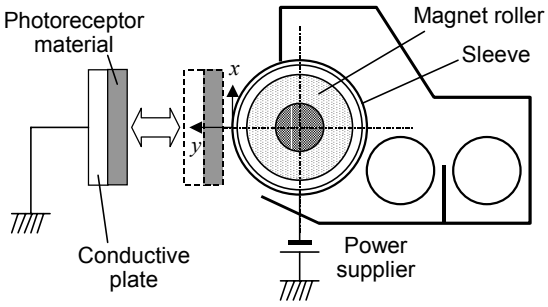


*Figure 4. Experimental setup using magnet roller.*

**Magnet Roller System**

Figure 4 shows another experimental setup with a magnet roller. In this experiment, non-spherical, soft magnetic, and conductive carriers without toner particles were provided on the magnet roller. The carriers are 35-80 μm in diameter, 5000 kg/m$^3$ in volume density, 0.400 kg/m$^2$ mass of unit area, and 11.5 in relative magnetic permeability. A grounded conductive flat plate with a photoreceptor layer of 25 μm thickness was set close to the sleeve with 350 μm gap. After the application of DC bias voltage to the sleeve, the plate was moved away from the sleeve to measure the amount of carrier beads attached on the photoreceptor surface.

The magnetic flux density distribution near the gap between the plate and the sleeve can be approximated by $B'(x, y) = (\alpha_1 x^2+\alpha_2 x+\alpha_3 x)/(\beta_1 y^2+\beta_2 y+\beta_3)$, in the Cartesian coordinate system $(x, y)$. The values of the coefficient $\alpha_1$, $\beta_1$, etc. were determined by regression of measured flux density distribution and the results are listed in Table 1.

**Table 1. Coefficient of magnetic flux density.**

| Coefficient | $B'_x$ | $B'_y$ |
|---|---|---|
| $\alpha_1$ | 0.0 | $-1.47\times10^{5}$ |
| $\alpha_2$ | $6.56\times10^{2}$ | 6.23 |
| $\alpha_3$ | $-2.09\times10^{-1}$ | 2.48 |
| $\beta_1$ | $1.00\times10^{6}$ | $9.97\times10^{5}$ |
| $\beta_2$ | $1.13\times10^{4}$ | $1.20\times10^{4}$ |
| $\beta_3$ | $1.76\times10^{1}$ | $1.96\times10^{1}$ |

## Numerical Method

**Applied Force to Carrier Bead**

Magnetic bonding force and electrostatic pull-off force are dominant forces applied to the magnetic and conductive carriers in development area. These forces are illustrated in Fig. 5. If the electrostatic force exceeds magnetic force, the top of the chain will be separated. In this study, these two forces are focused and calculated. The DEM[2,4] were employed to simulate chain forming process to estimate magnetic force. Electric field calculations were conducted on these simulated chains to estimate electrostatic force.

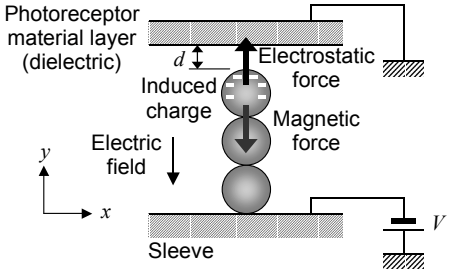


*Figure 5. Applied forces to carrier beads in development area.*

**Magnetic Force**

In the DEM calculation, the following momentum equation is solved for each carrier bead.

$$m_j \ddot{\boldsymbol{u}}_j = \boldsymbol{F}_j , \qquad (1)$$

where $m_j$, $\boldsymbol{u}_j$ and $\boldsymbol{F}_j$ are mass, displacement vector, and applied force vector to the $j$-th bead. Mechanical contact

force, magnetic force, air drag, and gravitational force are included in the applied force, while van der Waals force and electrostatic force were neglected. The mechanical contact force in the normal direction at the contact point was estimated from the Hertzian theory. The force in the tangential direction was assumed to be proportional to the normal force with a proportional constant 0.25.

The magnetic force $\boldsymbol{F}_{mj}$ to the $j$-th bead with the magnetic dipole moment $\boldsymbol{p}_j$ are given by the following expression under the assumption that each bead behaves as a magnetic dipole placed at the center of the bead.[5]

$$\boldsymbol{F}_{mj} = (\boldsymbol{p}_j \cdot \nabla)\boldsymbol{B}_j . \tag{2}$$

The magnetic flux density $\boldsymbol{B}_j$ at the position of the $j$-th bead and magnetic moment $\boldsymbol{p}_j$ are

$$\boldsymbol{B}_j = \boldsymbol{B}_j' + \sum_{\substack{k=1 \\ j \neq k}}^{N} \frac{\mu_0}{4\pi} \left( \frac{3(\boldsymbol{p}_k \cdot \boldsymbol{r}_{kj})}{|\boldsymbol{r}_{kj}|^5} \boldsymbol{r}_{kj} - \frac{\boldsymbol{p}_k}{|\boldsymbol{r}_{kj}|^3} \right), \tag{3}$$

$$\boldsymbol{p}_j = \frac{4\pi}{\mu_0} \frac{\mu - 1}{\mu + 2} \frac{a_j^3}{8} \boldsymbol{B}_j , \tag{4}$$

where $N$ is the number of particles, $\mu_0$ is the permeability of free space, $\mu$ is the relative permeability of beads, $a_j$ is the diameter of the $j$-th bead and $\boldsymbol{r}_{kj}$ is the position vector from the $k$-th to the $j$-th bead.

**Electrostatic Force**

The electrostatic force to pull-off beads can be estimated by the product of the field intensity near the top of chains and the charge of the beads. The electric field and induced charge were calculated by the following two equations, the Gauss's low and the conservation of charge, with the Finite Element Method.

$$\nabla \cdot (\varepsilon \nabla \phi) = -\rho , \ \nabla \cdot (\sigma \nabla \phi) = -\frac{\partial \rho}{\partial t} , \tag{5}$$

where $\phi$ is potential, $\varepsilon$, $\sigma$ and $\rho$ is permittivity, conductivity and space charge, respectively.

## Results and Discussion

**Solenoid Coil System**

Measured critical electric field intensities are plotted in Fig. 6. The field was simply estimated by $V/d$, where $V$ is applied voltage and $d$ is a gap between the top of the chain and the upper electrode. The electric field to break chains increases nonlinearly with the increase in coil current and increases with the increase in diameter. The dependencies correspond to the magnetic bonding force expressed by Eqs. (2)-(4).

Figure 7 shows the comparison of calculated magnetic force and electrostatic force. The magnetic force was calculated on a straight single chain as shown in Fig. 5 and the electrostatic force was obtained by the electric field calculation around chains using measured critical voltage. These two kinds of forces are supposed to balance at the moment when a chain is broken. In the figure, a straight line indicates the relation that the calculated magnetic force is equal to the measured critical electrostatic force. It is clearly recognized that the electrostatic forces and magnetic forces show good correlation even though they do not agree quantitatively. The result supports the validity of the BCO mechanism shown in Fig. 5. However, more accurate estimation is required for the quantitative discussion.

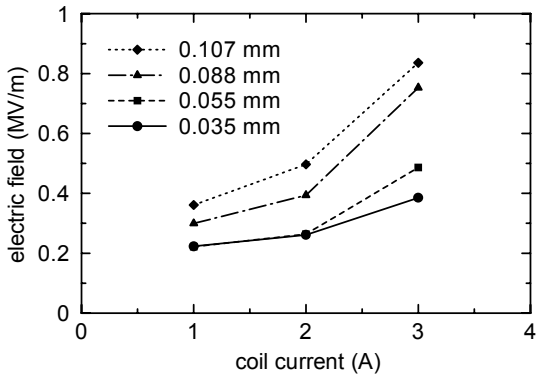


*Figure 6. Critical electric field to break chains.*

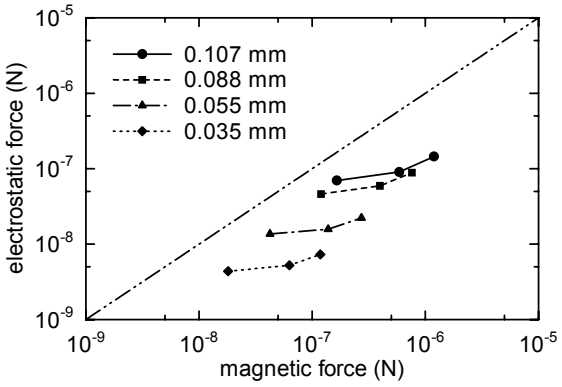


*Figure 7. Comparison of electrostatic and magnetic forces.*

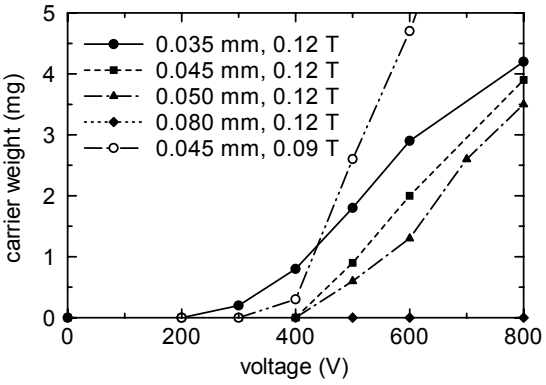


*Figure 8. Weight of electrically pulled-off carrier beads. The values indicated in the figure are bead diameters and maximum magnetic flux densities.*

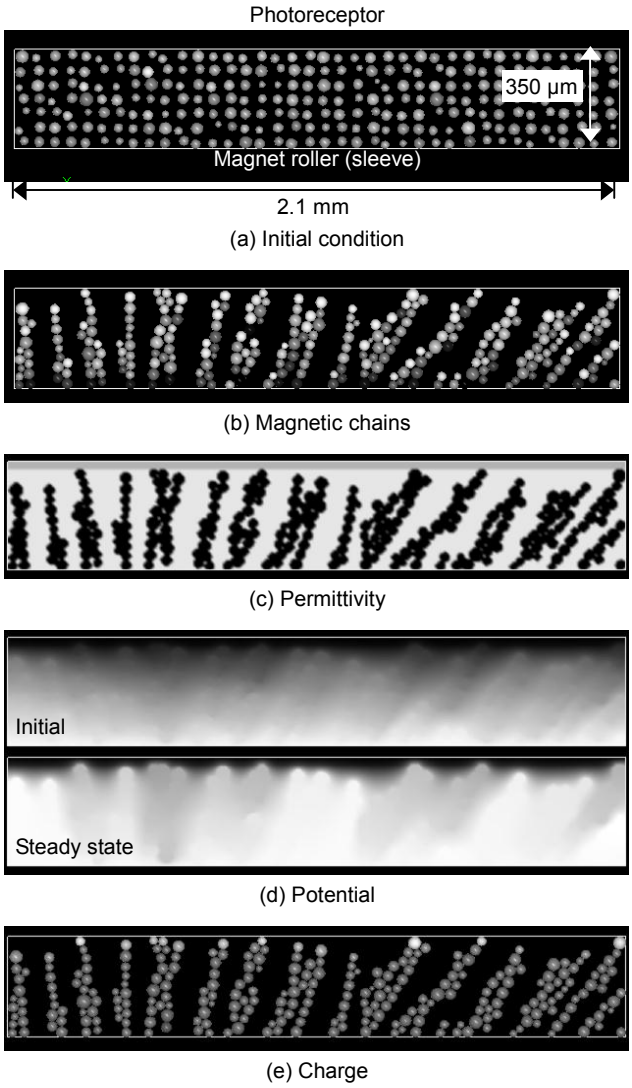


*Figure 9. Numerical results of chain forming process and electric field calculation.*

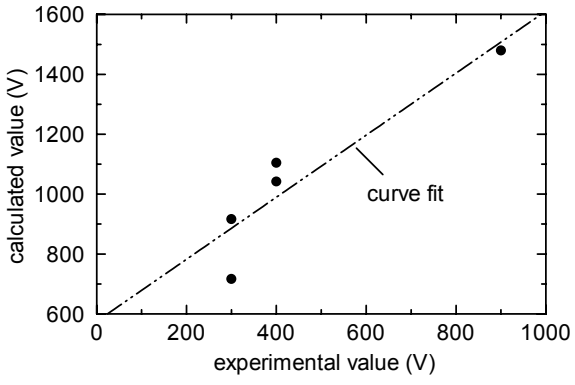


*Figure 10. Correlation of calculated and experimental critical pull-off voltage.*

**Magnet Roller System**

Figure 8 shows how the weight of electrically pulled-off carrier beads in the setup with the magnet roller were increased to the applied voltage between the roller and the plate for several kinds of bead diameters and two kinds of rollers. There exists critical voltage to separate chains and the weight of pulled-off carriers increase with the increase in applied voltage. The critical voltage and the increase rate of weight of carriers depend on diameters and magnetic flux densities. The results agree qualitatively with the results obtained in the solenoid coil experiment.

Figure 9 shows numerical results of chain forming process and electric field calculation in the normal condition, that is, beads in 35 µm diameter and 0.12 T in maximum magnetic flux density. Figure 9 (a) is an initial condition of the calculation. The center of the figure corresponds to the closest point between magnet roller and plate shown in Fig. 4. In this case, 266 carrier beads were distributed in the calculation domain. Figure 9 (b) shows calculated chain profiles at 1 ms after applying magnetic field specified by the values listed in Table 1. In Fig. 9 (b), gray level of each carrier bead indicates the magnitude of *y*-component of magnetic force. At the top of the chains, magnetic forces toward the magnetic roller were applied to the beads.

Figure 9 (c) is permittivity distribution for finite element electric field calculation. In the model, the properties of the elements where the carrier chains existed were set at 10 in relative dielectric constant and $6.61\times10^{-8}$ S/m in conductivity. Photoreceptor layer is assumed to be 3.0 in dielectric constant. Figure 9 (d) shows potential distributions in the initial condition and the steady state. In the stable condition, potential is uniform inside of bulk chain. As a result, the carrier bead at the top of each chain charged negatively as illustrated in Fig. 9 (e). Here in Fig. 9 (e), charge distribution of carrier beads are indicated by the gray levels of beads.

From the numerical calculation, critical pull-off voltages were estimated and values were compared to experimental values to confirm the validity of the method. Figure 10 shows the result and it also shows acceptable correlation of these values. A further study is required to resolve the cause of the over estimation in calculated results.

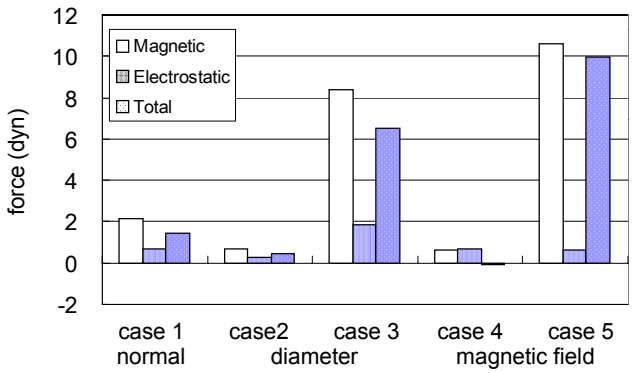


*Figure 11. Calculated magnetic, electrostatic and total forces.*

The effects of carrier diameter and magnetic field on the applied forces were investigated by the same procedure mentioned above. The results are shown in Fig. 11. In case 2 and 4, 1/2 of the normal values were assumed for diameter and magnetic field. In case 3 and 5, two times larger values were assumed. Same as the results in the solenoid coil experiment, the diameter and the magnetic field affect pull-off characteristics.

## Conclusion

In this study, electrostatic pull-off phenomenon known as BCO was investigated by two kinds of experiments and the numerical calculation. From the electrostatic pull-off measurement, it was clarified how the critical pull-off field intensity to break chains and the amount of pulled-off carriers depended on the bead diameter and the magnetic field. Magnetic bonding force and electric pull-off force were estimated numerically to discuss these experimental results. It was clarified that the bead-carry-out phenomenon can be predicted qualitatively from the comparison of calculated magnetic and electrostatic force.

## References

1. E. M. Williams, *The Physics and Technology of Xerographic Processes*, Krieger Publishing, FL, 1993.
2. N. Nakayama, H. Kawamoto and M. Yamaguchi, Statics of Magnetic Bead Chain in Magnetic Field, *J. Imaging Sci. Technol.*, **46**, 5 (2002), 422-428.
3. H. Kawamoto, N. Nakayama, S. Yamada and A. Sasakawa, Resonance Frequency and Stiffness of Magnetic Bead Chain in Magnetic Field, *IS&T's NIP18: The 18th International Conf. on Digital Printing Technologies*, (2002), 28-35.
4. P. A. Cundall and O. D. L. Strack, A Discrete Numerical Model for Granular Assemblies, *Géotechnique*, **29**, 1 (1979), 47-65.
5. R. S. Paranjpe and H. G. Elrod, Stability of Chains of Permeable Spherical Beads in an Applied Magnetic Field, *J. Appl. Phys.*, **60**, 1 (1986), 418-422.

## Biography

**Nobuyuki Nakayama** holds a BS degree in Physics from Tohoku Univ. (1983) and a Dr. degree in Mechanical Engineering from Waseda Univ. (2003). In 1983, he joined Fuji Xerox, and has been engaged in the research of electrophotography as a Researcher. From 2003, he has also been a Associate Researcher of Department of Mechanical Engineering, Waseda Univ. He is a member of the Imaging Society of Japan and the Japan Society of Mechanical Engineering.